Mixed-Valence Structures

Visualization of Local Valence Structures in Quasi-One-Dimensional Halogen-Bridged Complexes $[Ni_{1-x}Pd_x(chxn)_2Br]Br_2$ by STM**

Shinya Takaishi, Hitoshi Miyasaka, Ken-ichi Sugiura, Masahiro Yamashita,* Hiroyuki Matsuzaki, Hideo Kishida, Hiroshi Okamoto, Hisaaki Tanaka, Kazuhiro Marumoto, Hiroshi Ito, Shin-ichi Kuroda, and Tomohide Takami*

One-dimensional (1D) electron systems have been attracting much attention because many characteristic physical properties have been observed, such as the spin-density wave (SDW)

[*] Dr. S. Takaishi, Dr. H. Miyasaka, Prof. K.-i. Sugiura, Prof. M. Yamashita
Department of Chemistry, Graduate School of Science
Tokyo Metropolitan University and CREST (JST)
1-1 Minamiosawa, Hachioji, Tokyo 192-0397 (Japan)
Fax: (+81) 426-77-2525
E-mail: takaishi@comp.metro-u.ac.jp
yamashit@comp.metro-u.ac.jp

H. Matsuzaki, Dr. H. Kishida, Prof. H. Okamoto
Department of Advanced Material Science
Graduate School of Frontier Science
The University of Tokyo, Kashiwa, Chiba 277-8561 (Japan)

Dr. H. Tanaka, Dr. K. Marumoto, Prof. H. Ito, Prof. S. Kuroda
Department of Applied Physics, Graduate School of Engineering
Nagoya University, Furocho, Chikusa-ku
Nagoya, Aichi 464-8603 (Japan)

T. Takami
Visionarts Research Inc.
5-3-22 Minami-aoyama, Minato-ku, Tokyo 107-0062 (Japan)

[**] This work was partly supported by a Grant-in-Aid for Creative Scientific Research from the Ministry of Education, Culture, Sports, Science, and Technology. chxn = (1*R*,2*R*)-diaminocyclohexane.

 DOI: 10.1002/ange.200453905

and charge-density wave (CDW) in organic conductors,[1] soliton, polaron, and bipolaron states in π-conjugated polymers,[2] and slow relaxation of magnetization in several ferro- or ferrimagnetic compounds.[3] Quasi-1D halogen-bridged complexes are also attractive materials because of their marked physical properties such as intense and dichroic intervalence charge-transfer bands,[4] overtone progression of resonance Raman spectra,[5] luminescence spectra with large Stokes shifts,[6] large third-order nonlinear optical properties, and midgap absorptions attributable to solitons and polarons,[7] as well as providing 1D model compounds of high critical temperature (T_c) copper oxide superconductors.[8]

Theoretically, these MX chains are considered as Peierls–Hubbard systems where the electron–phonon interaction (S), the electron transfer (T), and the intra- and intersite Coulomb repulsion energies (U and V, respectively) compete or cooperate with each other.[9] The Pt and Pd compounds form CDW or mixed-valence states represented as $-X\cdots M^{2+}\cdots X-M^{4+}-X\cdots$ as a result of the electron–phonon interaction, where the bridging halogen atoms are displaced from the midpoints between the neighboring two metal ions.[10] Accordingly, the half-filled metallic band splits into the occupied valence band and unoccupied conduction band with finite Peierls energy gaps. Therefore, these compounds belong to class II of the Robin–Day classification for mixed-valence complexes.[11] On the other hand, the Ni complexes form Mott–Hubbard states expressed as $-X-Ni^{3+}-X-Ni^{3+}-X^-$ as a result of the strong electron correlation (U), where the bridging halogen atoms are located at the midpoints between two neighboring Ni ions.[12] Therefore, these Ni complexes belong to class III of the Robin–Day classification.[11] Very strong antiferromagnetic interactions among the spins located on the $Ni^{III}d_{z^2}$ orbitals through the bridging halogen ions are observed.[13] These Ni complexes have also been of recent interest in applied science because the largest third-order, nonlinear optical susceptibility of 10^{-4} esu has been observed in $[Ni(chxn)_2Br]Br_2$ (chxn: (1*R*,2*R*)-diaminocyclohexane).[14]

Recently, the mixed-metal complexes $[Ni_{1-x}Pd_x(chxn)_2Br]Br_2$ $(0 \le x \le 1)$ were synthesized.[15] The valence structures of these complexes are interesting because competition between the Ni^{3+}-Ni^{3+} Mott–Hubbard and Pd^{2+}-Pd^{4+} CDW states can be expected in single crystals. The electronic states of these complexes have been studied by infrared spectroscopy,[16] magnetic susceptibility,[17] and X-ray diffuse scattering.[18] According to these studies, the valence structure of the complexes with $x < 0.8$ form Mott–Hubbard states, whereas the complexes with $x > 0.8$ show CDW states. However, no information on local structures was obtained. In addition, it is difficult to clarify the valence structures, so an X-ray crystal structure analysis cannot be applied to such mixed-metal compounds. A scanning tunneling microscope (STM) is a powerful tool for studying local electronic structures in such compounds. Day described the usefulness of the method for halogen-bridged complexes in 1985.[19] Herein, we report the first visualized local valence structures in Ni-Pd mixed-metal complexes obtained by STM.

Figure 1 a shows an STM image of $[Ni(chxn)_2Br]Br_2$ in the range 200 × 200 Å. Bright spots in the image are observed

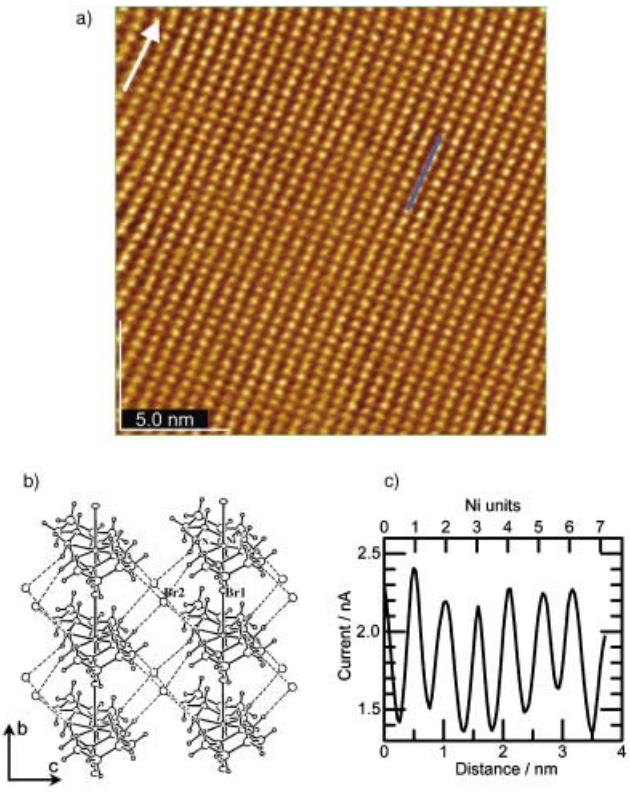

Figure 1. a) STM image of $[Ni(chxn)_2Br]Br_2$ on the *bc* plane (200 × 200 Å). The image was acquired with a sample bias of $V_s = +1.3$ V. The white arrow shows the 1D chain direction. b) Crystal structure of $[Ni(chxn)_2Br]Br_2$. c) Tunnel current profile of $[Ni(chxn)_2Br]Br_2$ on the blue line in Figure 1 a.

every 5 × 7 Å. The crystal structure of $[Ni(chxn)_2Br]Br_2$ is shown in Figure 1 b. The Ni···Ni distances along the *b* (1D chain) and *c* axes are 5.16 and 7.12 Å, respectively,[12] and hence these spots reflect the periodicity of $\{Ni(chxn)_2\}$ units in the *bc* plane. To investigate the valence structure in detail we plotted a current profile along the 1D chain (on the blue line) in Figure 1 c. The maximum of the current is observed every Ni unit, which indicates that all the Ni centers are equivalent and in the Mott–Hubbard Ni^{3+}-Ni^{3+} state in $[Ni(chxn)_2Br]Br_2$. This finding is consistent with the result obtained by single-crystal X-ray analysis.

An STM image in the range 200 × 200 Å and the crystal structure of $[Pd(chxn)_2Br]Br_2$ are shown in Figure 2 a and b, respectively. Bright spots are observed every 10 × 7 Å. The Pd···Pd distances along the *b* (1D chain) and *c* axes are 5.29 and 7.07 Å, respectively,[10] and thus these spots in the image reflect the twofold periodicity of the valence structure that result from to the CDW structure of $[Pd(chxn)_2Br]Br_2$. The phase of the CDW is almost aligned in the *bc* plane, which is consistent with the X-ray diffuse scattering study.[18] Therefore, correctly speaking, $[Pd(chxn)_2Br]Br_2$ should be formulated as $[Pd^{II}(chxn)_2][Pd^{IV}(chxn)_2Br_2]Br_4$.

Schematic band structures of $[Ni(chxn)_2Br]Br_2$ and $[Pd(chxn)_2Br]Br_2$ are shown in Figure 3. According to X-ray photoelectron spectra (XPS) and Auger spectra, the d_{z^2} band of Ni splits into occupied lower-Hubbard (LH) and unoccu-

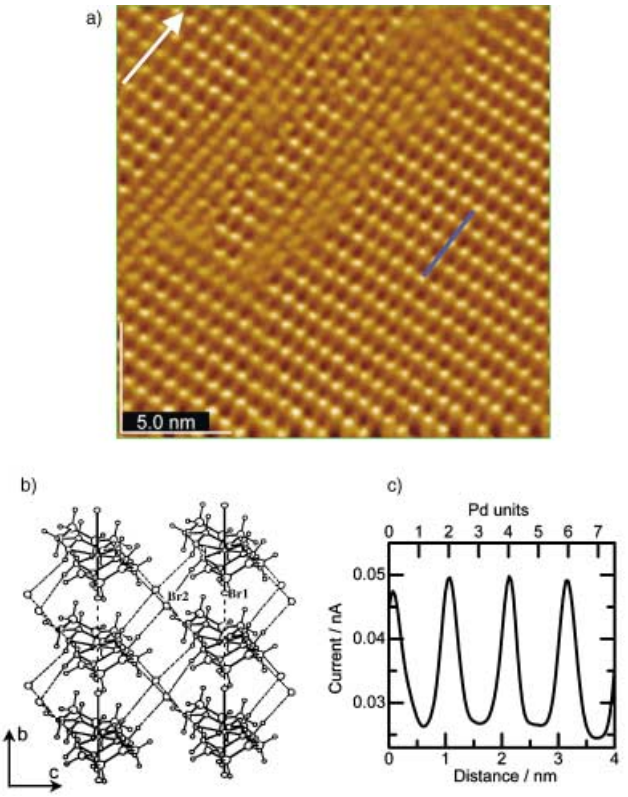

Figure 2. a) STM image of $[Pd(chxn)_2Br]Br_2$ on the *bc* plane (200×200 Å). The sample bias was $V_s = +1.0$ V. The 1D chain direction is shown by a white arrow. b) Crystal structure of $[Pd(chxn)_2Br]Br_2$. c) Current profile of $[Pd(chxn)_2Br]Br_2$ on the blue line in Figure 2a.

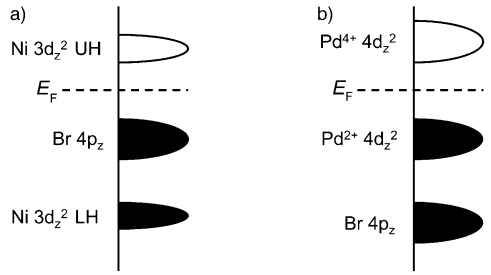

Figure 3. Schematic band structures of a) $[Ni(chxn)_2Br]Br_2$ and b) $[Pd(chxn)_2Br]Br_2$.

pied upper-Hubbard (UH) bands as a consequence of the strong electron correlation and, as a result, the valence and conduction bands of $[Ni(chxn)_2Br]Br_2$ are the p_z band of bridging Br atoms and the UH band composed of the d_{z^2} orbital of Ni, respectively.[20] In $[Pd(chxn)_2Br]Br_2$, on the other hand, the valence and conduction bands are the d_{z^2} bands of Pd^{2+} and Pd^{4+}, respectively. As the STM measurements were performed with positive sample bias, the tunnel current is observed from the Fermi energy (E_F) of a tip to a conduction band of the sample. Therefore, in $[Ni(chxn)_2Br]Br_2$, the tunnel current from E_F to the UH d_{z^2} band of Ni^{3+} is observed, whereas that from E_F to the d_{z^2} band of Pd^{4+} is observed in $[Pd(chxn)_2Br]Br_2$, which affords the twofold periodicity along the 1D chain observed in the STM image.

Next, we made STM measurements on the mixed-metal complexes $[Ni_{1-x}Pd_x(chxn)_2Br]Br_2$ to determine their local valence structure. Figure 4 shows the STM images of the

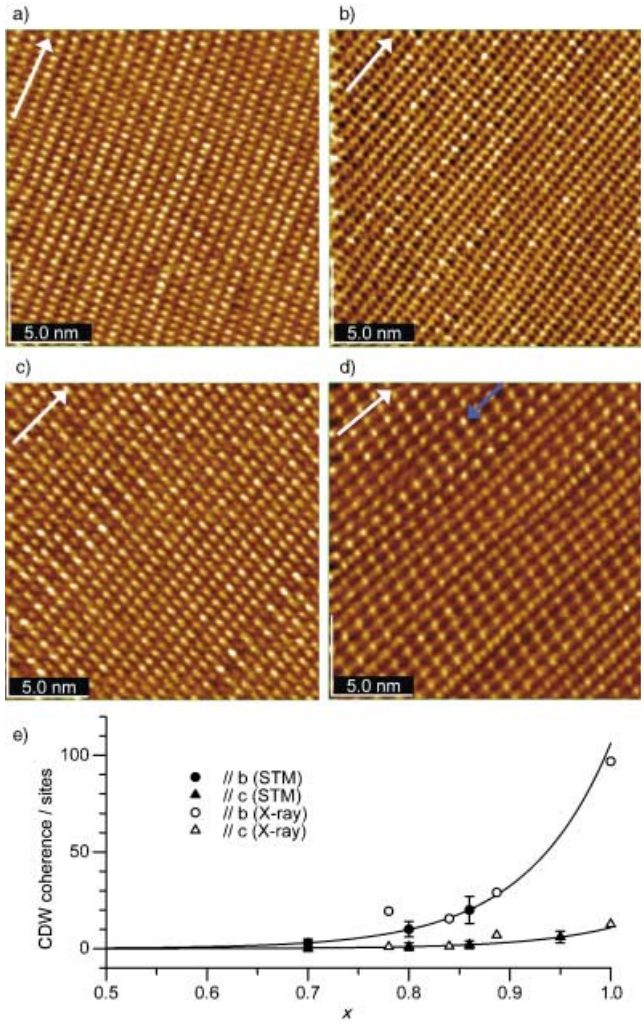

Figure 4. STM images of $[Ni_{1-x}Pd_x(chxn)_2Br]Br_2$ with a) $x = 0.70$, b) $x = 0.80$, c) $x = 0.86$, and d) $x = 0.95$ on the *bc* plane (200×200 Å). The sample bias was $V_s = +1.0$ V. The 1D chain directions are shown as white arrows; the blue arrow shows the 1D chain on which the spin soliton is observed. e) CDW coherence as a function of *x*. The filled circle and triangle represent CDW coherence along the chain and *c* axis, respectively, determined by STM measurement. The empty circle and triangle represent those determined by X-ray diffuse scattering measurements reported by Wakabayashi et al. The solid lines are guides to the eye.

complex with a) $x = 0.70$, b) $x = 0.80$, c) $x = 0.86$, and d) $x = 0.95$ in an area of 200×200 Å. In the $x = 0.70$ complex (Figure 4a), an image similar to that of $[Ni(chxn)_2Br]Br_2$ is observed, with almost no twofold periodicity. This result shows that the $x = 0.70$ complex forms almost in the Mott–Hubbard state, where the oxidation state of the Pd center is 3+. In the $x = 0.80$ complex (Figure 4b), on the other hand, twofold periodicity is observed in several areas, which is

attributable to the CDW state. This CDW state has coherence over approximately 10 metal sites along the *b* axis, but almost no coherence along the *c* axis. In the $x = 0.86$ complex (Figure 4c), the CDW coherence is clearly more propagated than that of the $x = 0.80$ complex. In the $x = 0.86$ complex, CDW coherence spreads over approximately 20 metal sites along the *b* axis, and 2 or 3 metal sites along the *c* axis. Figure 4d shows the STM image of the $x = 0.95$ complex. A large part of this image has a twofold periodicity, that is, a CDW state. Along the *b* axis, a large part of the chains with a CDW state conserve the twofold periodicity within the measured length (ca. 40 metal sites), which shows that the CDW coherence along the chain is longer than 20 nm. Along the *c* axis, on the other hand, CDW coherence spreads over approximately 6 or 7 sites. We plotted the CDW coherent length as a function of *x* in Figure 4e together with the data evaluated by X-ray diffuse scattering measurements reported by Wakabayashi et al.[18] The CDW coherence determined by STM measurements is in good agreement with the X-ray diffuse scattering results. It was revealed that CDW coherence is generated slightly from about $x = 0.70$ and increasingly propagated with increasing value of *x*.

In addition, the phase of the CDW on the chain shown as a blue arrow in Figure 4d is reversed within the chain. This reverse can be recognized as the generation of a spin soliton. A schematic chain structure with the spin soliton in a CDW complex is shown together with *trans*-polyacetylene (*trans*-PA) in Figure 5. It is well established that the spin soliton in

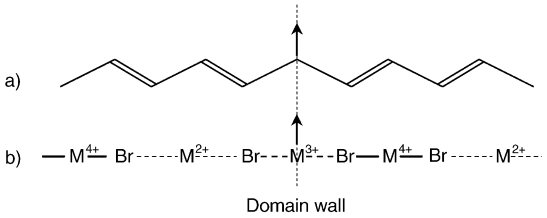

Figure 5. Schematic chain structure of the spin soliton in a) *trans*-polyacetylene and b) halogen-bridged CDW complexes.

trans-PA is made by a domain wall originating from the mismatch of the phase of alternating bonds.[2] On the other hand, it has been revealed that spin solitons in the CDW complexes are made by mismatch of the CDW phase, and M^{3+} sites act as domain walls.[13,21] This domain wall of the spin soliton observed in Figure 4d spreads over approximately 10 metal sites, which is consistent with theoretical prediction.[22] Although the mechanism of the spin soliton in the complex is the same as that in *trans*-PA, the most marked difference between them is the activation energy for soliton motion. This energy has been evaluated as about 80 meV by light-induced ESR studies,[21] which is much larger than that of *trans*-PA (2 meV).[23] This finding shows that soliton motion in $[Pd(chxn)_2Br]Br_2$ is much slower than that of *trans*-PA. As a result, the spin soliton has a lifetime of the order of a minute, so it can be observed by STM, which operates on the millisecond-order timescale. Although spin solitons are well known in π-conjugated polymers,[2,23] this is the first time the spin soliton has been visualized in real space.

In summary, we have visualized the Mott–Hubbard and CDW states in quasi-1D halogen-bridged Ni and Pd complexes, respectively. In addition, we succeeded in visualizing the propagation of CDW coherence and the spin soliton in real space in the mixed-metal complexes $[Ni_{1-x}Pd_x(chxn)_2Br]Br_2$ for the first time.

Experimental Section

Single crystals of $[Ni_{1-x}Pd_x(chxn)_2Br]Br_2$ ($x = 0$, 0.70, 0.80, 0.86, 0.95, and 1.0) were synthesized according to previous studies.[16] The elemental ratio of Ni and Pd was determined by ICP emission measurements with a SEIKO SPS 7000 plasma spectrometer. STM measurements were performed at room temperature and ambient pressure. Single crystals of $[Ni_{1-x}Pd_x(chxn)_2Br]Br_2$ were cut and mounted on a sample stage with carbon paste so that the surface of the *bc* plane could be observed. All STM images were acquired in the constant height mode using a JEOL JSPM-5200 microscope. A positive sample bias voltage (V_s) was used.

Received: February 2, 2004 [Z53905]

Keywords: bridging ligands · coordination modes · mixed-valent compounds · scanning probe microscopy · valence structures

[1] a) A. Andrieux, D. Jerome, K. Bechgaard, *J. Phys. Lett.* **1981**, *42*, 87–90; b) L. Forro, S. Bouffard, J. P. Pouget, *J. Phys. Lett.* **1984**, *45*, 453–459.
[2] a) I. B. Goldberg, H. R. Crowe, P. R. Newman, A. J. Heeger, A. G. MacDiarmid, *J. Chem. Phys.* **1979**, *70*, 1132–1136; b) W. P. Su, J. R. Schrieffer, A. J. Heeger, *Phys. Rev. B* **1980**, *22*, 2099–2111.
[3] a) A. Caneschi, D. Gatteschi, N. Lalioti, C. Sangregorio, R. Sessoli, G. Venturi, A. Vindigni, A. Rettori, M. G. Pini, M. A. Novac, *Angew. Chem.* **2001**, *113*, 1810–1813; *Angew. Chem. Int. Ed.* **2001**, *40*, 1760–1763; b) R. Clérac, H. Miyasaka, M. Yamashita, C. Coulon, *J. Am. Chem. Soc.* **2002**, *124*, 12837–12844; c) R. Lescouezec, J. Vaissermann, C. Ruiz-Perez, F. Lloret, R. Carrasco, M. Julve, M. Verdaguer, Y. Dromzee, D. Gatteschi, W. Wernsdorfer, *Angew. Chem.* **2003**, *115*, 1521–1524; *Angew. Chem. Int. Ed.* **2003**, *42*, 1483–1486.
[4] a) M. Tanaka, S. Kurita, T. Kojima, Y. Yamada, *Chem. Phys.* **1984**, *91*, 257–265; b) Y. Wada, T. Mitani, M. Yamashita, T. Koda, *J. Phys. Soc. Jpn.* **1985**, *54*, 3143–3153.
[5] a) R. J. H. Clark, M. L. Franks, W. R. Trumble, *Chem. Phys. Lett.* **1976**, *41*, 287–292; b) R. J. H. Clark, *Adv. Infrared Raman Spectrosc.* **1983**, *11*, 95–130.
[6] H. Tanino, K. Kobayashi, *J. Phys. Soc. Jpn.* **1983**, *52*, 1446–1456.
[7] a) H. Okamoto, T. Mitani, K. Toriumi, M. Yamashita, *Phys. Rev. Lett.* **1992**, *69*, 2248–2251; b) H. Okamoto, M. Yamashita, *Bull. Chem. Soc. Jpn.* **1998**, *71*, 2023–2039.
[8] M. Yamashita, K. Yokoyama, S. Furukawa, T. Manabe, T. Ono, K. Nakata, C. Kachi-Terajima, F. Iwahori, T. Ishii, H. Miyasaka, K. Sugiura, H. Matsuzaki, H. Kishida, H. Okamoto, H. Tanaka, Y. Hasegawa, K. Marumoto, H. Ito, S. Kuroda, *Inorg. Chem.* **2002**, *41*, 1998–2000.
[9] a) D. Baeriswyl, A. R. Bishop, *J. Phys. C* **1988**, *21*, 339–356; b) A. Mishima, K. Nasu, *Phys. Rev. B* **1989**, *40*, 5593–5597.
[10] A. Hazell, *Acta Crystallogr. Sect. C* **1991**, *47*, 962–966.
[11] M. B. Robin, P. Day, *Adv. Inorg. Chem. Radiochem.* **1967**, *9*, 247–422.
[12] K. Toriumi, Y. Wada, T. Mitani, S. Bandow, M. Yamashita, Y. Fujii, *J. Am. Chem. Soc.* **1989**, *111*, 2341–2342.

[13] H. Okamoto, K. Toriumi, T. Mitani, M. Yamashita, *Phys. Rev. B* **1990**, *42*, 10381 – 10387.
[14] H. Kishida, H. Matsuzaki, H. Okamoto, T. Manabe, M. Yamashita, Y. Taguchi, Y. Tokura, *Nature* **2000**, *405*, 929 – 932.
[15] T. Manabe, M. Yamashita, T. Kawashima, H. Okamoto, H. Kitagawa, T. Mitani, K. Toriumi, H. Miyamae, K. Inoue, K. Yakushi, *Proc. SPIE Int. Soc. Opt. Eng.* **1997**, *3145*, 106 – 115.
[16] M. Yamashita, T. Ishii, H. Matsuzaka, T. Manabe, T. Kawashima, H. Okamoto, H. Kitagawa, T. Mitani, K. Marumoto, S. Kuroda, *Inorg. Chem.* **1999**, *38*, 5124 – 5130.
[17] K. Marumoto, H. Tanaka, S. Kuroda, T. Manabe, M. Yamashita, *Phys. Rev. B* **1999**, *60*, 7699 – 7702.
[18] Y. Wakabayashi, N. Wakabayashi, M. Yamashita, T. Manabe, N. Matsushita, *J. Phys. Soc. Jpn.* **1999**, *68*, 3948 – 3952.
[19] P. Day, *Philos. Trans. R. Soc. Lond. Ser. A* **1985**, *314*, 131 – 144.
[20] H. Okamoto, Y. Shimada, Y. Oka, A. Chainani, T. Takahashi, H. Kitagawa, T. Mitani, K. Toriumi, K. Inoue, T. Manabe, M. Yamashita, *Phys. Rev. B* **1996**, *54*, 8438 – 8445.
[21] H. Tanaka, K. Marumoto, S. Kuroda, M. Yamashita, *Synth. Met.* **2003**, *135–136*, 317 – 318.
[22] K. Iwano, *J. Phys. Soc. Jpn.* **1999**, *68*, 935 – 940.
[23] B. R. Weinberger, E. Ehrenfreund, A. Pron, A. J. Heeger, A. G. MacDiarmid, *J. Chem. Phys.* **1980**, *72*, 4749 – 4755.

